

ROLE OF THE HIERARCHY OF COHERENT STRUCTURES IN THE TRANSPORT OF SOLID PARTICLES IN TURBULENT CHANNEL FLOW AT HIGH REYNOLDS NUMBERS

Yutaro Motoori

Graduate School of Engineering Science
Osaka University
1-3 Machikaneyama, Toyonaka, Osaka, 560-8531, Japan
y.motoori.es@osaka-u.ac.jp

Susumu Goto

Graduate School of Engineering Science
Osaka University
1-3 Machikaneyama, Toyonaka, Osaka, 560-8531, Japan
s.goto.es@osaka-u.ac.jp

ABSTRACT

To investigate the transport of heavy small particles (inertial particles) in high-Reynolds-number wall turbulence, we conduct direct numerical simulations of inertial particles in turbulent channel flow at the friction Reynolds number $Re_\tau = 2000$. The Reynolds number is higher than the one analysed in our previous study (Motoori *et al.*, 2022). In the statistically steady state, particles distribute inhomogeneously; particles with different relaxation times form voids and clusters with different sizes in the bulk of the flow. To explore the origin of the multiscale voids and clusters of particles, we objectively identify the axes of tubular vortices. These identifications enable us to quantitatively show that vortices sweep out the particles of the relaxation time comparable with their turnover time, irrespective of their size and existing height. This explains the reason why the multiscale clusterings are well described in terms of the local Stokes number defined by the turnover time of multiscale vortices. The results obtained by the present study are consistent with our previous study (Motoori *et al.*, 2022), and the description of the particle transport leads to understanding velocity statistics and wall-deposition mechanism of inertial particles in high-Reynolds-number wall turbulence.

INTRODUCTION

We investigate the motion of rigid spherical particles in turbulent channel flow at a high Reynolds number. In particular, we focus on heavy small particles, which are sometimes called inertial particles. When the particles are sufficiently smaller than the Kolmogorov length, and the mass density of the particles is much larger than that of fluid, the particles are governed by

$$\frac{d\mathbf{x}_p}{dt} = \mathbf{u}_p \quad \text{and} \quad \frac{d\mathbf{u}_p}{dt} = -\frac{k_p}{\tau_p} (\mathbf{u}_p - \mathbf{u}). \quad (1)$$

Here, \mathbf{x}_p and \mathbf{u}_p are the position and velocity of particles, and \mathbf{u} is the fluid velocity at the particle position. Particles are

subjected only to the Stokes drag with the nonlinear correction $k_p = 1 + 0.15Re_p^{0.687}$, where Re_p is the particle Reynolds number. We emphasize that the motion of pointwise particles is characterized only by the particle velocity relaxation time τ_p .

In wall-bounded turbulence, it is known that inertial particles governed by (1) tend to accumulate in the near-wall region. Many studies (e.g. Soldati & Marchioli, 2009) on inertial particles dispersed in low-Reynolds-number wall-turbulence have revealed the role of the buffer-layer coherent structures in the wall-accumulation process. However, as the Reynolds number increases, larger-size structures emerge in addition to the near-wall ones. Their roles in the transport of inertial particles remain unclear. Meanwhile, our recent study (Motoori & Goto, 2021) revealed the generation mechanism of the hierarchy of multiscale vortices in turbulent channel flow at the friction Reynolds number $Re_\tau = 4179$. Recently, we investigated how inertial particles are transported in turbulent channel flow based on the hierarchy of flow coherent structures (Motoori *et al.*, 2022). The key to these studies is the extraction of the hierarchical structures in real space.

In the present study, we examine the details of the transport of inertial particles based on the hierarchy of vortices for the higher Reynolds number turbulence. For this purpose, we newly conduct the direct numerical simulations (DNS) of the dispersion of inertial particles in turbulent channel flow at $Re_\tau = 2000$. The Reynolds number is higher than in the turbulent channel flow ($Re_\tau = 1000$) examined in our previous study (Motoori *et al.*, 2022). In the present paper, we visualize the spatial distributions of particles and the hierarchy of vortices, and also we quantitatively show the relation between them.

DIRECT NUMERICAL SIMULATIONS

We numerically simulate turbulent channel flow at $Re_\tau = 2000$ driven by a constant pressure gradient by solving the Navier-Stokes equations of an incompressible fluid. Since the target of the present study is a dilute dispersion of small particles, we neglect their effect on fluid motion. The temporal

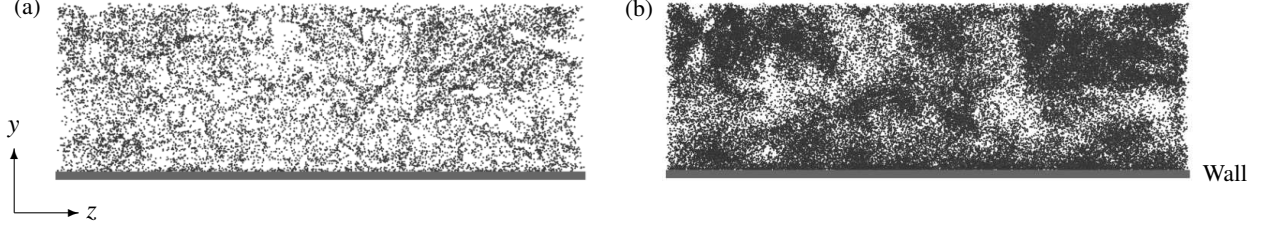


Figure 1. Two-dimensional (y - z) spatial distributions of inertial particles with (a) $St_+ = 25$ and (b) 250 within a layer of thickness 200 wall units. The clusters and voids of particles are larger for larger St_+ .

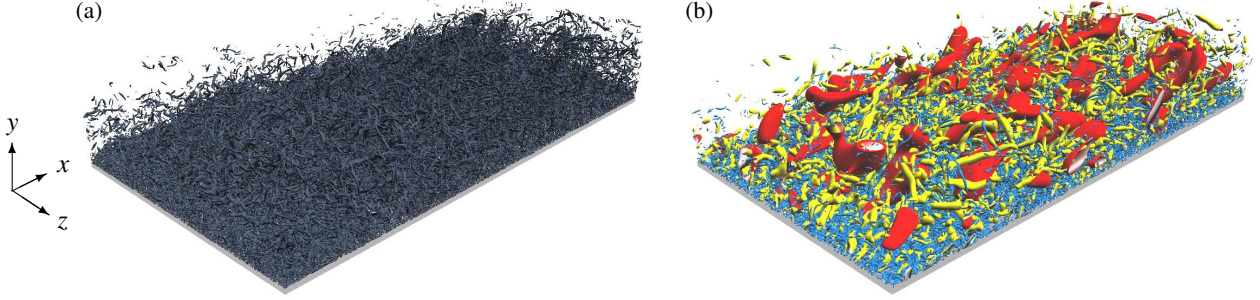


Figure 2. (a) Smallest-scale vortices identified by the isosurfaces of the second invariant Q of the velocity gradient tensor. (b) Hierarchy of vortices identified by the isosurfaces of the second invariant $Q^{(\sigma)}$ of the scale-decomposed velocity gradient tensor at scales $\sigma^+ = 480$ (red), 120 (yellow) and 30 (blue). We visualize a subdomain (half in the wall-normal direction) of the computational domain.

integrations of the viscous and convection terms are made by using the second-order Crank-Nicolson method and the third-order Adams-Bashforth method, respectively. For the spatial discretization of the terms in the governing equations, we use a sixth-order central difference scheme on a staggered grid in the streamwise (x) and spanwise (z) directions and a non-uniform finite difference scheme in the wall-normal (y) direction. The numbers of grid points are $(N_x \times N_y \times N_z) = (3072 \times 1536 \times 1536)$. The numerical simulation method is the same as that used by our previous study (Motoori *et al.*, 2022) but the present Reynolds number is higher than in the previous one ($Re_\tau = 1000$).

We track 10^7 particles by numerically integrating (1) by the second-order Adams-Bashforth method. We assume that the diameter of particles is sufficiently small so that $Re_p = 0$. As mentioned in the introduction, the most important parameter is the particle relaxation time τ_p , which is expressed in nondimensional form as the Stokes number. We use the Stokes number $St_+ = \tau_p/\tau_+$ nondimensionalized by the wall-unit time-scale $\tau_+ (= \nu/u_\tau^2)$, where u_τ is the friction velocity and ν is the kinematic viscosity. We examine seven cases with $St_+ = 1, 10, 25, 50, 100, 250$ and 1000, which are the same parameters in Bernardini (2014) and Motoori *et al.* (2022). For the following analyses, we take the average in the statistically steady state.

CLUSTERING OF PARTICLES

We show in figure 1 the two-dimensional (y - z) spatial distributions of particles with (a) $St_+ = 25$ and (b) 250 in the steady state. We visualize only particles in a thin (200 wall units) layer. The important observation is that particles form clusters and that the size of the voids is larger for larger St_+ . This multiscale nature was quantitatively verified by the pair

correlation function in turbulent channel flow at $Re_\tau = 1000$ (Motoori *et al.*, 2022). To understand the formation mechanism of the multiscale clustering, we quantitatively investigate the relationship between the clustering of particles and the hierarchy of vortices. For this purpose, in the next section, we identify the hierarchy of vortices in turbulent channel flow.

IDENTIFICATION OF MULTISCALE VORTICES

To extract vortical structures, we show in figure 2(a) the isosurface of the second invariant Q of the velocity gradient tensor. In this figure, we can only observe fine tubular vortices. This is because the smallest-scale vortices determine the velocity gradients. Therefore, to capture the hierarchy of vortices, we need a scale decomposition.

To extract the hierarchy of vortices in turbulence, we use a band-pass filter, which was also used in Motoori & Goto (2021) and Motoori *et al.* (2022). In this method, we first apply the Gaussian filter with the filter scale σ to the fluctuating velocity \tilde{u}_i . Since the obtained velocity $u_i^{(\sigma)low}$ contains the information of all the scales larger than σ , the filter corresponds to a low-pass filter of the Fourier modes of the velocity. We then take the difference between the low-pass filtered fields at two different scales, i.e. $u_i^{(\sigma)}(\mathbf{x}) = u_i^{(\sigma)low}(\mathbf{x}) - u_i^{(2\sigma)low}(\mathbf{x})$. This filter corresponds to a band-pass filter of the Fourier modes in the sense that $u_i^{(\sigma)}$ has the contributions only from around the scale σ .

To identify the hierarchy of vortices, we evaluate scale-decomposed second invariant $Q^{(\sigma)}$ of the velocity gradient tensor from $u_i^{(\sigma)}$. Figure 2(b) shows positive isosurfaces of $Q^{(\sigma)}$ at scales $\sigma^+ = 30, 120$ and 480, where \cdot^+ denotes the wall units nondimensionalized by u_τ and ν . The isosurfaces indeed capture vortices with the filter scale σ (see also figure 2

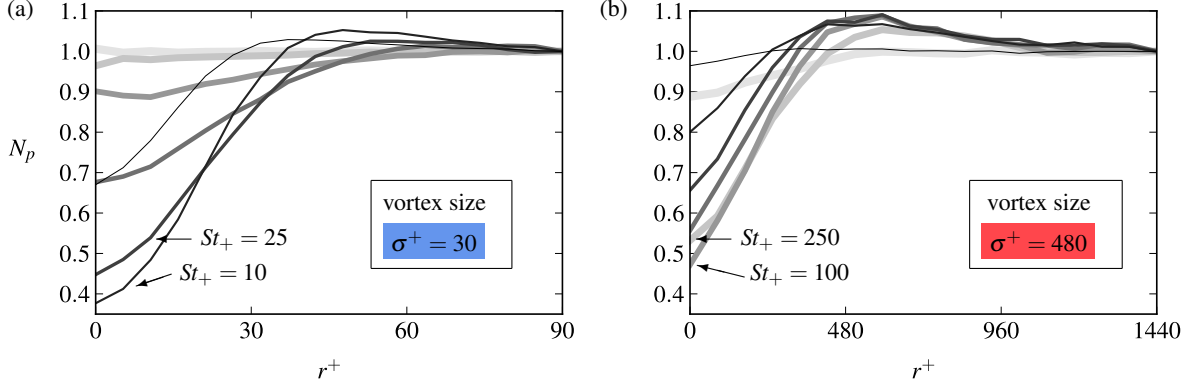


Figure 3. Average number N_p of inertial particles existing at distance r from an axis of vortices with sizes (a) $\sigma^+ = 30$ and (b) 480 in the layers (a) $500 \lesssim y^+ < 1000$ and (b) $1500 \lesssim y^+ < 2000$. The values are normalized by those at $r = 3\sigma$. From the thinner (and darker) to the thicker (and lighter) lines, $St_+ = 1, 10, 25, 50, 100, 250$ and 1000. (a) Vortices with size $\sigma^+ = 30$ tend to sweep out particles with $St_+ = 10$, whereas (b) those with $\sigma^+ = 480$ sweep out particles with $St_+ = 100$ and 250.

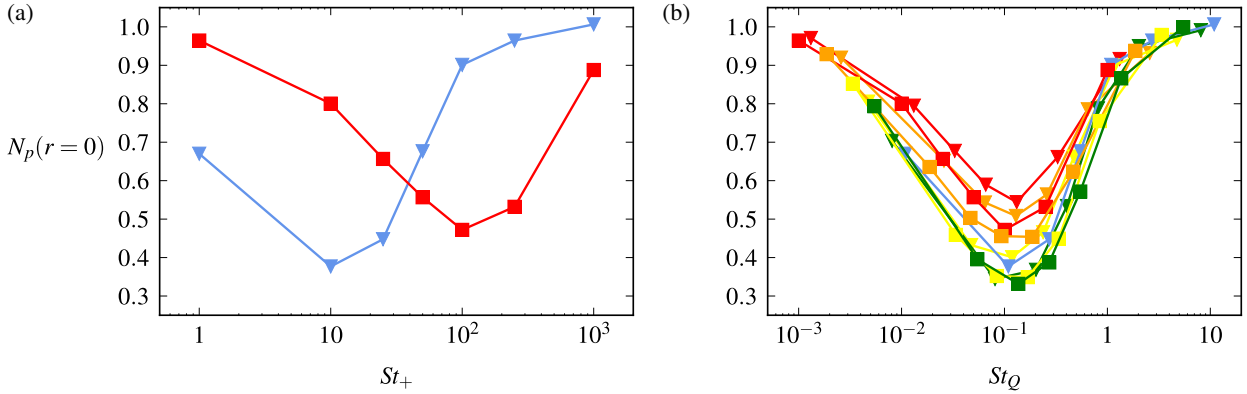


Figure 4. (a) Average number $N_p(r=0)$ of inertial particles on the axes of vortices, namely, the values at $r = 0$ shown in figure 3. In (b), we show $N_p(r=0)$ for the several cases: the different sizes [$\sigma^+ = 30$ (blue), 60 (green), 120 (yellow), 240 (orange) and 480 (red)], and different layers [$500 \lesssim y^+ < 1000$ (triangles), and $1500 \lesssim y^+ < 2000$ (squares)]. The values are shown as functions of (b) St_Q instead of (a) St_+ . Here, we use the value of τ_Q at the centre of each layer.

in Motoori & Goto, 2021). Here, $\sigma^+ = 30$ is of the order of size of the smallest-size vortices, whereas $\sigma^+ = 480$ is approximately the largest-size vortices. Moreover, by applying the low-pressure method (Miura & Kida, 1997) to the band-pass filtered fields, we objectively identify the axes of tubular vortices (see figure 3 in Motoori *et al.*, 2022). In the following, we use the axes for the examination of the spatial distribution of particles around vortices at different sizes.

PARTICLE DISTRIBUTION AROUND VORTICES

To quantitatively show the origin of clusters of particles, we use the identified vortex axes. This enables us to evaluate the number of particles around the axis of each vortex. For example of the results obtained by the present study, we show the number density N_p of particles as a function of the distance r for $y^+ \gtrsim 500$.

We first show, in figure 3, the normalized N_p for particles around the axes of small-scale vortices ($\sigma^+ = 30$; see blue vortices in figure 2b) existing in the layer $500 \lesssim y^+ \lesssim 1000$. Here, we normalize N_p so that $N_p < 1$ when particles are sparsely distributed; whereas $N_p > 1$, when they form clusters. The thinner (and darker) lines indicate particles with smaller St_+ . Looking at the second thinnest line ($St_+ = 10$), the number

ratio takes the minimum at $r = 0$, whereas it takes the maximum around for $\sigma \lesssim r \lesssim 2\sigma$. This tendency is also observed for particles with another Stokes number ($St_+ = 25$) close to $St_+ = 10$. On the other hand, the number of particles with larger $St_+ (\gtrsim 100)$ is almost constant, irrespective of r . Hence, in the layer $500 \lesssim y^+ \lesssim 1000$, the small-size ($\sigma^+ = 30$) vortices most likely to sweep out particles with $St_+ \approx 10$. This is consistent with the observation (figure 1a) that particles form small-size clusters in the instantaneous field.

Figure 3(b) shows N_p around vortices with a larger size $\sigma^+ = 480$ within the layer $1500 \lesssim y^+ < 2000 (= h^+)$. We can see that particles with $St_+ = 100$ and 250 are swept out from the large ($\sigma^+ = 480$) vortices to form a cluster around them.

We replot, in figure 4(a), N_p at $r = 0$ as a function of St_+ . Note that the blue triangles show the results for $\sigma^+ = 30$ in the layers $500 \lesssim y^+ \lesssim 1000$, whereas the red squares show those for $\sigma^+ = 480$ in the layers $1500 \lesssim y^+ \lesssim 2000$. In other words, these symbols show the values at $r = 0$ shown in figure 3. The lines do not collapse. This means that different-size and different-height vortices do contribute to the clustering of particles in different ranges of St_+ . More precisely, vortices at larger sizes or those further from the wall tend to sweep out particles with larger St_+ ; note that the well of red line shifts to larger St_+ . This suggests that vortices sweep out particles of

the relaxation time similar to their eddy turnover time, because larger-size vortices have longer eddy turnover time.

To verify this, we define the eddy turnover time $\tau_Q(\sigma, y)$ of vortices with size σ at height y in terms of the root-mean-square $Q_{rms}^{(\sigma)}(y)$ of the second invariant tensor of the velocity gradient tensor at the size σ . We then define the local Stokes number by

$$St_Q(\sigma, y) = \frac{\tau_p}{\tau_Q(\sigma, y)}, \quad (2)$$

where $\tau_Q = 1/\sqrt{Q_{rms}^{(\sigma)}(y)}$. The vertical values in figure 4(b) are the same as in (a) but are shown as functions of St_Q instead of St_+ . In addition to the two results shown in figure 4(a), we investigate the cases for vortices with different sizes and heights, and we show in figure 4(b) all the results together. It is most important to observe that the well of all the lines collapses around $St_Q \approx 0.2$. We can therefore conclude that, irrespective of the height and size, vortices preferentially sweep out particles of the relaxation time τ_p comparable with the turnover time τ_Q . This observation around wall-detached ($\sigma < y$) vortices is similar to that in homogeneous turbulence (Yoshimoto & Goto, 2007; Oka & Goto, 2021).

In summary, in the log and outer layers of turbulent channel flow, the origin of the multiscale clustering is the hierarchy of vortices. More concretely, vortices most effectively sweep out particles of the relaxation time comparable with their turnover time irrespective of their size, their existing height and the Reynolds number. Incidentally, we showed the clustering near the wall is also explained in terms of the hierarchy of wall-attached quasi-streamwise vortices and low-speed streaks (Motoori *et al.*, 2022). From the present results, irrespective of the Reynolds number, we may infer that wall-attached structures contribute most significantly to transporting particles with the relaxation time comparable with their turnover time of the vortices.

CONCLUSIONS

To investigate the transport mechanism of inertial particles in high-Reynolds-number turbulent channel flow, we have

conducted DNS of those with seven relaxation times ($St_+ = 1-1000$) in the turbulence at $Re_\tau = 2000$. The key ingredient of our analysis is the objective identification of the hierarchy of coherent vortices. We have shown the distribution of particles around the axes of vortices at each level of the hierarchy. The analyses lead to the main conclusion: vortices sweep predominantly particles with the relaxation times comparable with their turnover time. Hence, the clustering of particles is determined by the local Stokes number ($St_Q \approx 0.2$) irrespective of the size and height of coherent vortices (figure 4b).

REFERENCES

- Bernardini, M. 2014 Reynolds number scaling of inertial particle statistics in turbulent channel flows. *Journal of Fluid Mechanics* **758**, R1.
- Miura, H. & Kida, S. 1997 Identification of tubular vortices in turbulence. *Journal of the Physical Society of Japan* **66**, 1331–1334.
- Motoori, Y. & Goto, S. 2021 Hierarchy of coherent structures and real-space energy transfer in turbulent channel flow. *Journal of Fluid Mechanics* **911**, A27.
- Motoori, Y., Wong, C. & Goto, S. 2022 Role of the hierarchy of coherent structures in the transport of heavy small particles in turbulent channel flow. *Journal of Fluid Mechanics* (in press).
- Oka, S. & Goto, S. 2021 Generalized sweep-stick mechanism of inertial-particle clustering in turbulence. *Physical Review Fluids* **6**, 044605.
- Soldati, A. & Marchioli, C. 2009 Physics and modelling of turbulent particle deposition and entrainment: Review of a systematic study. *International Journal of Multiphase Flow* **35**, 827–839.
- Yoshimoto, H. & Goto, S. 2007 Self-similar clustering of inertial particles in homogeneous turbulence. *Journal of Fluid Mechanics* **577**, 275–286.